NOVA SCHOOL OF SCIENCE & TECHNOLOGY

PHYSICS DEPARTMENT

PEDRO MIGUEL COIMBRA RIBEIRO

BSc in Biochemistry

Cytotoxicity of Electrospun mats loaded with antimicrobial agents towards Macrophages

MASTERS IN BIOMATERIALS AND NANOMEDICINE

NOVA University of Lisbon

OCTOBER 2023

NOVA SCHOOL OF SCIENCE & TECHNOLOGY

Physics Department

Cytotoxicity of electrospun mats loaded with antimicrobial agents towards Macrophages

PEDRO MIGUEL COIMBRA RIBEIRO

BSc in Biochemistry

Supervisor: Jorge Carvalho Silva,
Professor Associado, Universidade NOVA de Lisboa

Co-adviser: Tânia Vieira,
Investigadora, Universidade NOVA de Lisboa

Examination Committee:

Chairperson: Doutor João Paulo Miranda Ribeiro Borges, Professor Catedrático na Faculdade Nova de Lisboa;

Rapporteur: Doutora Luísa Isabel Serra Glória Fialho, Investigadora Contratada no Instituto de Investigação e Inovação em Saúde da Universidade do Porto

Supervisor: Doutor Jorge Alexandre Monteiro Carvalho Silva, Professor Associado na Faculdade de Ciências e Tecnologias da Universidade Nova de Lisboa

MASTER IN BIOMATERIALS AND NANOMEDICINE

Universidade NOVA de Lisboa
OCTOBER 2023

Cytotoxicity of electrospun mats loaded with antimicrobial agents towards macrophages.

Copyright © Pedro Miguel Coimbra Ribeiro, Faculdade de Ciências e Tecnologia, Universidade NOVA de Lisboa.

A Faculdade de Ciências e Tecnologia e a Universidade NOVA de Lisboa têm o direito, perpétuo e sem limites geográficos, de arquivar e publicar esta dissertação através de exemplares impressos reproduzidos em papel ou de forma digital, ou por qualquer outro meio conhecido ou que venha a ser inventado, e de a divulgar através de repositórios científicos e de admitir a sua cópia e distribuição com objetivos educacionais ou de investigação, não comerciais, desde que seja dado crédito ao autor e editor.

.

AGRADECIMENTOS

Este trabalho foi feito com muito esforço e trabalho árduo, que me fez crescer não só em conhecimento, mas também como pessoa. Ao longo deste caminho pude contar com algumas pessoas, a quem gostaria de agradecer:

Em primeiro lugar, ao Professor Doutor Jorge Carvalho, orientador desta dissertação, obrigado pela disponibilidade, orientação e pela partilha de conhecimento e experiência científica, sempre patentes durante todo o desenvolvimento deste trabalho.

À Doutora Tânia Vieira, coorientadora desta dissertação, obrigada pela hospitalidade, disponibilidade prestadas durante o desenvolvimento deste trabalho especialmente pelos conhecimentos adquiridos e também pela paciência.

Quero agradecer também aos meus companheiros de laboratório, João, Sofia e á Catarina Correia, com eles o trabalho de laboratório pareceu leve, tranquilo e até divertido.

Obrigado pelo apoio que os meus amigos me deram nesta última jornada académica da minha vida.

E gostaria também de agradecer à minha namorada Maria João Fartaria Borges pelo apoio incondicional durante os tempos de escrita, que sem ela teriam sido muito mais stressantes.

Por último, mas não menos importante, à minha família, especialmente á minha irmã e aos meus pais, que foram sem dúvida, o maior pilar que tive nesta fase e em toda a minha.

“It's not about how much we have lost, it's about we have left.” (Unknown).

ABSTRACT

New developments in nanotechnology have transformed wound treatment by introducing materials with better absorption and antimicrobial properties. Biocompatible nanoparticles, like gold (Au), silver (Ag), and zinc (Zn), have become promising candidates for promoting wound healing. This research used a chemical reduction method to create Au, Ag, and Zn nanoparticles. Additionally, nanofibers were made using electrospun solutions consisting of polycaprolactone (PCL), chitosan (CS), and gelatine (GEL), which included varying amounts of nanoparticles and antiseptics like povidone-iodine (PVP-I), chlorhexidine (CHX), and octenidine dihydrochloride (OCT). The study examined these nanoparticles, polymer-based materials, and antiseptics in detail, highlighting their various interactions. The findings have significant implications for biomedical science, antimicrobial applications, and the development of biomaterials. Among the nanoparticles studied, AuNPs stood out as excellent candidates for applications that require precise particle sizes with remarkable uniformity. ZnONPs also showed size uniformity, while AgNPs were slightly less consistent but still within acceptable ranges. Further analysis using scanning electron microscopy (SEM) and dynamic light scattering (DLS) revealed how various additives affected fibre morphology within PCL and GEL mats. Some additives led to better fibres, while others created broader distributions of fibre diameters. In chitosan (CS) mats, cross-linking reduced fibre diameter without compromising mat structure, and additives had minimal impact on fibre morphology. Cytotoxicity tests showed that some formulations were non-cytotoxic while others had varying degrees of cytotoxicity. Finally, the antibacterial properties of AgNPs, AuNPs, and ZnONPs against *E. coli* were tested, with AgNPs showing promise in fighting bacterial infections, especially at lower concentrations.

Keywords: metallic nanoparticles, macrophages, anti-septic agents, electrospinning, cytotoxicity.

RESUMO

Novos desenvolvimentos na nanotecnologia transformaram o tratamento de feridas através da introdução de materiais com melhores propriedades de absorção e antimicrobianas. As nanopartículas biocompatíveis, como o ouro (Au), a prata (Ag) e o zinco (Zn), tornaram-se candidatos promissores para promover a cicatrização de feridas. Esta investigação utilizou um método de redução química para criar nanopartículas de Au, Ag e Zn. Além disso, foram produzidas nanofibras utilizando soluções electrfiadas constituídas por policaprolactona (PCL), quitosano (CS) e gelatina (GEL), que incluíam quantidades variáveis de nanopartículas e anti-sépticos como iodopovidona (PVP-I), clorexidina (CHX) e dicloridrato de octenidina (OCT). O estudo examinou em pormenor estas na-nopartículas, materiais à base de polímeros e anti-sépticos, destacando as suas várias interacções. Os resultados têm implicações significativas para a ciência biomédica, as aplicações antimicrobianas e o desenvolvimento de biomateriais. Entre as nanopartículas estudadas, as AuNPs destacaram-se como excelentes candidatos para aplicações que requerem tamanhos de partículas precisos com uma uniformidade notável. As ZnONPs também mostraram uniformidade de tamanho, enquanto as AgNPs foram um pouco menos consistentes, mas ainda dentro de faixas aceitáveis. Análises posteriores utilizando microscopia eletrónica de varrimento (SEM) e dispersão dinâmica da luz (DLS) revelaram como os vários aditivos afectaram a morfologia das fibras nos tapetes de PCL e GEL. Alguns aditivos conduziram a fibras mais finas, enquanto outros criaram distribuições mais alargadas de diâmetros de fibras. No que diz respeito às fibras do quitosano (CS), a reticulação reduziu o diâmetro das fibras sem comprometer a estrutura da membrana, e os aditivos tiveram um impacto mínimo na morfologia das fibras. Os testes de citotoxicidade mostraram que algumas formulações não eram citotóxicas, enquanto outras apresentavam graus variáveis de citotoxicidade. Por fim, foram testadas as propriedades antibacterianas das AgNPs, AuNPs e ZnONPs contra a *E. coli*, tendo as AgNPs demonstrado ser promissoras no combate a infecções bacterianas, especialmente em concentrações mais baixas.

Palavras chave: nanopartículas metálicas, macrófagos,agentes anti-sépticos, electrospinning, citotoxicidade.

LIST OF CONTENTS

AGRADECIMENTOS ..... **V**

ABSTRACT ..... **VII**

RESUMO ..... **IX**

LIST OF FIGURES ..... **XIII**

LIST OF TABLES ..... **XIV**

ABBREVIATIONS ..... **XV**

1 INTRODUCTION **1**

1.1.1 State of the art treatment for wound healing 1

1.1.2 Nanoparticles in Wound Healing 2

1.2 Polymers 2

1.2.1 Polymers: PCL 3

1.2.2 Polymers: CS 3

1.2.3 Polymers: GEL 3

1.3 Nanofiber matrices obtained by electrospinning 4

1.3.1 Electrospinning Process 4

1.4 Metal Oxide Nanoparticles 5

1.4.1 Silver Nanoparticles 6

1.4.1.1 Synthesis 6

1.4.1.2 Antimicrobial Activity 7

1.4.1.3 Toxicity 8

1.4.2 Gold Nanoparticles 8

1.4.2.1 Synthesis 9

1.4.2.2 Toxicity 9
1.4.2.3 Antimicrobial Activity 9
1.4.3 Zinc Oxide Nanoparticles 10
1.4.3.1 Synthesis 10
1.4.3.2 Toxicity 10
1.4.3.3 Antimicrobial Activity 11
1.5 Antiseptics 11
1.6 Macrophages Role in Wound Healing 12
1.6.1 Importance of Macrophages 12
1.7 Main Goals of this Project 12
2 MATERIALS AND METHODS 15
2.1 Nanoparticles Synthesis 15
2.1.1 Silver Nanoparticles Synthesis 15
2.1.2 Zinc Oxide Nanoparticles Synthesis 15
2.1.3 Gold Nanoparticles Synthesis 16
2.2 Dynamic Light Scattering 16
2.3 Electrospinning Procedure 16
2.4 Chemical Cross-Liking 17
2.5 SEM Analysis 18
2.6 Cytotoxicity 18
2.6.1 Resazurin Assay 19
3 RESULTS AND DISCUSSION 21
3.1 Nanoparticle Analysis 21
3.1.1 DLS 21
3.1.2 SEM 22
3.2 Nanofiber morphology analysis 23
3.2.1 SEM: Polycaprolactone (PCL) 23
3.2.2 SEM: Gelatine (GEL) 24
3.2.3 SEM: Chitosan (CS) 26
3.3 Cytotoxicity 27
3.3.1 Metallic Nanoparticles 27

3.3.2 Antiseptics 28
3.3.3 Polymeric Mats 29
3.3.3.1 Polycaprolactone (PCL) 29
3.3.3.2 Chitosan (CS) 30
3.3.3.3 Gelatine (GEL) 30
3.4 Antibacterial Activity 32
3.4.1 Minimum Inhibitory Concentration (MIC) 32
BIBLIOGRAPHY 34

LIST OF FIGURES

Figure 1.1: Polycaprolactone Chemical Structure 3
Figure 1.2: Chitosan Chemical Structure 3
Figure 1.3 Gelatine Chemical Structure 4
Figure 1.4 Illustration of the Electrospinning process [11] 5
Figure 1.5: The procedure for creating AgNPs. [13] 6
Figure 1.6: The mechanism of antimicrobial activity of AgNPs. [13] 8
Figure1.7: Process for the synthesis of AuNPs [15] 9
Figure 2.1: Resazurin reduction to resorufin to evaluate cell viability [26] 19
Figure 3.1: (A) Zinc Oxide (0,050mM) and (B)Silver Nanoparticles (29,50 mM) produced by chemical precipitation method on image using SEM 22
Figure 3.2: SEM images of PCL electrospun mats produced from: (A)PCL, (B)PCL+AgNPs, (C)PCL+ZnONPs, (D)PCL+PVP-I, (E)PCL+CHX, (F)PCL+OCT .... **Error! Bookmark not defined.**
Figure 3.3: SEM images of GEL electrospun mats produced from: (A)GEL before crossliking, (B)GEL after crosslinking, (C)GEL+AgNPs, (D)GEL+OCT, (E)GEL+CHX, (F)GEL+PVP-I, (G) GEL+ZnONPs ..... **Error! Bookmark not defined.**
Figure 3.4: SEM images of CS electrospun mats produced from: (A)CS before crosslinking, (B)CS after crosslinking, (C)CS+AgNPs, (D)CS+ZnONPs, (E)CS+OCT, (F)CS+CHX 26
Figure 3.5: Results of differentiated THP-1 cell's viability, obtained in cytotoxic test of metallic nanoparticles 27
Figure 3.6: Results of differentiated THP-1 cell's viability, obtained in cytotoxic test of Antiseptics . 28
Figure 3.7: Results of differentiated THP-1 cell's viability, obtained in cytotoxic test of pure PCL and PCL loaded with metallic NPs and antiseptics 29
Figure 3.8: Results of differentiated THP-1 cell's viability, obtained in cytotoxic test of pure CS and CS loaded with metallic NPs and antiseptics 30
Figure 3.9: Results of differentiated THP-1 cell's viability, obtained in cytotoxic test of pure GEL and GEL loaded with metallic NPs and antiseptics 31

LIST OF TABLES

Table 2.1: Polymers with antiseptics and respective deposition parameters 17
Table 2.2: Polymers with metallic nanoparticles and respective deposition parameters 17
Table 3.1: Metallic Nanoparticles measurements from DLS 21
Table 3.2: Average fibre diameter of ZnONPs and AgNPs obtained from SEM 22
Table 3.3: Average fibre diameter of PCL matrices obtained from SEM 24
Table 3.4: Average fibre diameter of GEL matrices obtained from SEM 25
Table 3.5: Average fibre diameter of CS matrices obtained from SEM 27
Table 3.6: MIC and MBC concentration values for *E.Coli* 32

ABBREVIATIONS

AgNPs – Silver nanoparticles
ATP – Adenosine Triphosphate
AuNPs – Gold nanoparticles
CHX – Chlorhexidine
CS - Chitosan
DLS – Dynamic Light Scattering
DMEM – Dulbecco Modified Eagle Medium
DMSO – dimethyl sulfoxide
DNA - deoxyribonucleic acid
ES - Electrospinning
MBC - Minimum Bacterial Concentration
MIC - Minimum Inhibitory Concentration
NPs – Nanoparticles
OCT – octenidine dihydrochloride
PBS – Phosphate Buffered saline.
PMA – phorbol 12-myristate-13-acetate
PVP – polyvinylpyrrolidone
PVP-I – povidone-iodine
RPMI – Roswell Park Memorial Institute
SEM – Scanning Electron Microscopy
TSB - Trypticase Soy Broth
ZnONPs – Zinc oxide nanoparticles
GTA – Glutaraldehyde

1 INTRODUCTION

1.1 Wound healing

Wound recovery aims to restore both structure and function of damaged tissue. The human body has a remarkable ability to repair wounds through a series of intricate cellular and molecular events. These wounds can result from various causes, including trauma, surgical interventions, and chronic conditions such as diabetes. Understanding the underlying mechanisms of wound healing and developing effective therapeutic strategies are paramount [1].

Over the years, significant advancements have been made in unravelling the complex cascade of events involved in wound healing. From the first inflammatory response to the later stages of cell proliferation, tissue formation, and remodelling, each phase is meticulously regulated by many signalling molecules, growth factors, and cellular interactions. However, despite the body's natural healing abilities, certain wounds show impaired healing processes, leading to chronic ulcers, infections, and substantial morbidity. Such scenarios need innovative approaches to hasten and enhance the healing process.

1.1.1 State of the art treatment for wound healing

Dealing with wound healing, particularly in cases of chronic non-healing wounds, can be a challenging process. [2], [3]. Innovations in wound care have resulted in the development of several state-of-the-art treatments that can enhance the healing process, such as:

- Bioactive wound dressing: these dressings comprise three types of matrices: synthetic matrix scaffolds, matrices derived from animals, and human tissue and help treat both non-healing wounds and acute wounds [2].
- Topical wound-healing products include a wide range of modalities that contain growth factors, antimicrobial agents, and dressings and effectively promote recovery [3].
- Mesenchymal Stem Cells (MSCs) therapy: MSCs have regenerative properties when combined with scaffolds, hydrogels, or matrices [4].

These advanced treatments offer hope for people with chronic non-healing wounds, promising options for easing the healing process. However, fully comprehend chronic wounds underlying pathologies and develop even more effective therapies is required more studies [2].

1.1.2 Nanoparticles in Wound Healing

There are numerous possibilities for nanoparticles (NPs) in the future since they can promote wound recovery. Even though NPs are used in wound healing, assuring their safety biologically is crucial before implementation. Skin irritation and allergies have been reported as harmful effects of NPs applied topically. Studies have shown that NP exposure can exacerbate inflammation, and psoriasis and cause oxidative stress, autophagy, and programmed cell death in fibroblasts and keratinocytes. The effects of NPs on health depend on several factors, including their size, shape, surface charge, stability, and concentration. Therefore, modifying the properties of newly developed NPs for wound treatment is essential to reduce harm towards skin cells. Stabilisers, substances that can increase stability and reduce dermatitis caused by NPs, like metal shells or polymers. Despite advancements in wound healing, challenges still need to be addressed, such as the potential for AgNPs and ZnONPs to cause haemolysis. Polysaccharides and phospholipids can be used to modify the surface of NPs and improve their physicochemical properties. Additionally, the distribution of NPs throughout the body and their potential impact on organ systems is of concern, leading to various defects [5].

1.2 Polymers

There are two types of polymers, synthetic and natural. The latter have gained significant attention for various applications. Synthetic polymers are not only man-made, but some can also have their origins in the petrochemical industry. There are concerning issues with petroleum-based polymers, such, as waste disposal, limited availability of petroleum, rising costs and might have a non-biodegradable nature.

Contrarily to synthetic polymers natural polymers hold appeal due to their cost effectiveness (low production costs), ready availability in nature, ability to degrade naturally in the environment and within human bodies (thus being environmentally friendly), biocompatibility with organisms, without causing harm or toxicity (as they consist of monosaccharides and amino acids). As a result, they have found use in the pharmaceutical and cosmetic fields since they structurally resemble biological macromolecules, and so are recognized by the organism. Nonetheless these natural polymers do come with a drawback. For instance, they are susceptible to environmental exposure from metals and microbes during production, which can result in contamination [6]. In this study, three polymers were used being them polycaprolactone (PCL), chitosan (CS), and gelatine (GEL).

1.2.1 Polymers: PCL

Figure 1.1 illustrates the chemical structure of PCL, which is a biodegradable polyester with a low melting point of approximately 60 ºC. This characteristic allows PCL to be easily fabricated into mats, films, and injection commodities. The process of preparing PCL involves ring-opening polymerisation of ε-caprolactone. [7].

PCL is a synthetic polymer that has a slow degradation rate and hydrophobic, making it an intriguing material for creating long-term implantable devices and drug delivery systems. Hydrolysis of ester linkages in physiological conditions is responsible for the degradation of PCL in wound dressings.

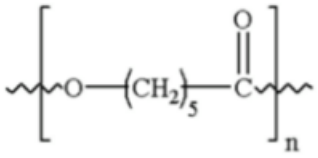

Figure 1.1: Polycaprolactone Chemical Structure.

1.2.2 Polymers: CS

Chitosan, shown in figure1.2, is a linear polysaccharide composed by deacetylation of chitin and consists of randomly distributed β-(1-4)-linked D-glucosamine and N-acetyl-D-glucosamine. It has better solubility in acidic environments. Due to its natural origin, chitosan may be susceptible to contamination by both inorganic and organic impurities. Nevertheless, chitosan is a biocompatible and biodegradable compound showing non-toxic properties. Furthermore, it showcases antibacterial and antifungal activities, useful in biomedicine [8].

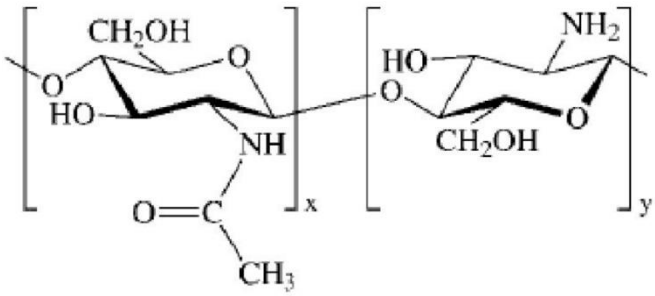

Figure 1.2: Chitosan Chemical Structure.

1.2.3 Polymers: GEL

Gelatine, as depicted in Figure 1.3, is also a naturally occurring polymer. GEL is obtained through the process of hydrolysing collagen found in animal skin, white connective tissue, and bones.

It primarily comprises glycine, proline, and 4-hydroxyproline residues. Notably, gelatine forms transparent, elastic, and thermos-reversible gels, which can be modified through chemical crosslinking.

This compound is highly biocompatible, well-tolerated by living organisms and minimises the risk of adverse reactions when used in tissue engineering. Its biodegradability is crucial for tissue engineering as it allows the scaffold material to be gradually replaced by the patient's tissue over time. This set of characteristics makes gelatine very regarded in tissue engineering [9].

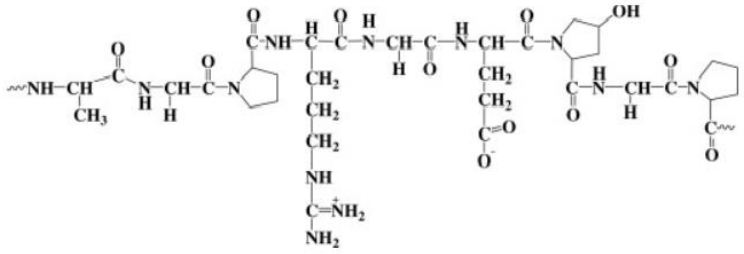

Figure 1.3 Gelatine Chemical Structure.

1.3 Nanofiber matrices obtained by electrospinning

Electrospinning (ES) is widely acknowledged as a convenient method for producing functional fibrous scaffolds. The performance and structure of electrospun nanofibers can be enhanced by incorporating active molecules in various ways. ES creates nanofibers that later find diverse applications ranging from filtration to biomedical uses, such as cancer therapy since they provide controlled drug release and ease chemotherapies delivery due to their high-loading capability, and wide surface area.

The electrospinning process is influenced by factors that fall into three categories: electrospinning parameters, solution characteristics, and environmental conditions. ES parameters include applied electric field, the spacing between the needle and collector, the flow rate, and the needle diameter. Solution-related factors include the choice of solvent, polymer concentration, viscosity, and solution conductivity. Environmental parameters comprise relative humidity and temperature. The mentioned factors directly contribute to generating smooth and bead-free fibre mats. To understand the electrospinning technique and polymeric nanofiber fabrication, it is crucial to have a comprehensive understanding of the governing parameters.

1.3.1 Electrospinning Process

In Figure 1.4, is described the standard setup used for electrospinning. This setup includes a high-voltage power source, a syringe, a spinneret (usually a needle with a rounded end), and a conductive collector. The power supply can be either direct current (DC) or alternating current (AC). The spinneret extrudes the solution during electrospinning, forming a droplet due to surface tension. When electricity is applied, the surface charges with the same sign create an electrostatic repulsion that causes the

droplet to transform into a Taylor cone. A charged jet is then released from the cone. At first, the jet travels straight but soon begin to whip and bend due to instability. As the jet is stretched into thinner diameters, it solidifies quickly and deposits fibres on the grounded collector. [10].

Nanofiber mats produced for skin applications can incorporate antiseptics that help the skin natural microflora to prevent the action of invading microorganisms, reducing the likelihood of infection. Therefore, matrices with antiseptic properties were developed and studied in this study. These biocidal properties can be obtained by incorporating either metallic nanoparticles, such as AgNPs, AuNPs, and ZnONPs, with antimicrobial characteristics or using antiseptics like the ones used in the study.

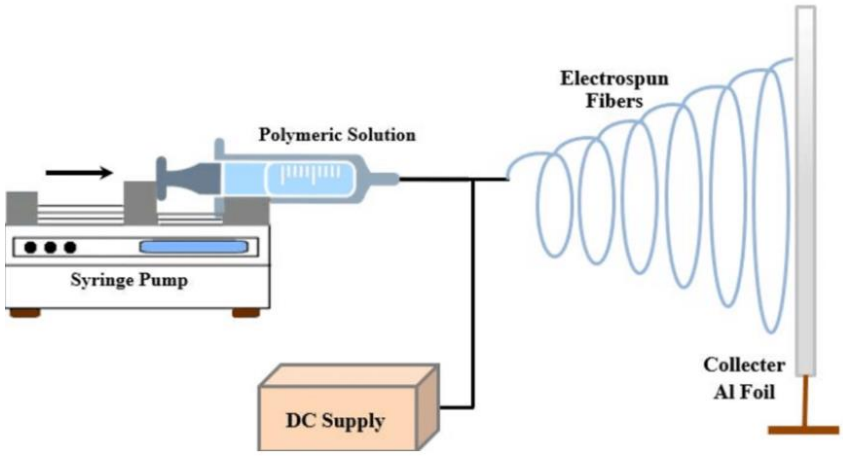

Figure 1.4 Illustration of the Electrospinning process [11].

1.4 Metal Oxide Nanoparticles

Metallic nanoparticles (NPs) have many benefits in the field of biomedicine and are widely used. In biomedical research, NPs are used for their various properties, such as their ability to be synthesized in different shapes and sizes. They can also be easily functionalized on the surface, making them highly compatible with biological systems. Additionally, they possess superior physicochemical properties. Two commonly used NPs are gold (AuNPs) and silver (AgNPs). AuNPs are frequently used in biosensing due to their unique optical properties and can be used as a nanocarrier for drug delivery. AgNPs, on the other hand, are primarily used as antimicrobial agents. They can exhibit antineoplastic activity when modified with a biocompatible polymer or targeted ligands. Zinc oxide nanoparticles (ZnONPs) have

properties that make them suitable for various applications, including drug delivery, antitumor, antibacterial, antidiabetic, and theragnostic tools. Nanoparticles made of metal and metal oxides exhibit promising abilities in combating bacterial strains.

Three theoretical mechanisms have been demonstrated for the metallic NPs antibacterial activity: first, the presence of the NPs on the membrane may alter its permeability, leading to the release of membrane proteins, lipopolysaccharides, and other biomolecules within the cell. Secondly, NPs generate reactive oxygen species (ROS), which lead to instigating oxidative impairment in cells. Lastly, microbes metabolising these NPs can decrease adenosine triphosphate (ATP) levels, disrupting DNA replication [5].

1.4.1 Silver Nanoparticles

The properties of silver nanoparticles (AgNPs), chemical stability, catalytic activity, localised surface plasma resonance, and high conductivity, have made them interesting. Research has shown that reactive oxygen species (ROS) present on the surface of AgNPs or released silver ions can lead to cell death in mammals and microbes. This unique property provides them with antibacterial and antifungal effects. As a result, applied topically, AgNPs show promising potential in preventing inflammation and promoting wound healing [12].

1.4.1.1 Synthesis

The chemical synthesis of AgNPs is cost-effective, easily scalable, and maintains a consistent size distribution compared to other methods. Among the available techniques, chemical reduction is the preferred approach to develop such nanosystems. The process involves the use of a metal precursor, reducing agents, and a stabilizing agent. The synthesis consists of two nucleation and growth stages (Figure 1.5). In this synthesis, the stabilizing agent can serve a dual purpose by also acting as a reducing agent.[13].

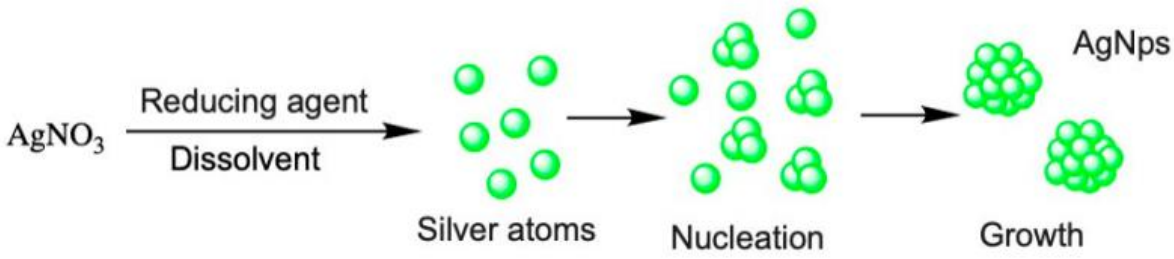

Figure 1.5: The procedure for creating AgNPs [13].

To achieve the specific size, consistency, and shape of AgNPs, it is crucial to have precise control over the nucleation phase. This requires careful monitoring of various experimental factors, such as the choice of precursor used in the reaction, the amount and type of reducing agents, the concentration of reagents, the pH levels, and the temperature. Stabilisation is essential in preventing agglomeration and oxidation processes in AgNPs synthesis. Consequently, one employed strategy involves stabilising agents that effectively protect against aggregation [13].

1.4.1.2 Antimicrobial Activity

AgNPs bactericidal effect can be explained by four primary mechanisms. Firstly, they are drawn to the bacterial surface. Secondly, they can interfere with the cell wall and membrane, resulting in changes to permeability. Thirdly, they can induce toxicity and oxidative stress by generating ROS and free radicals. Lastly, they can influence signal transduction pathways. Many authors describe the adhesion of AgNPs to the surface as the step in a complex process inhibiting bacterial growth. Both the size and zeta potential influence the AgNPs adhesion process. After having adhered to a surface, AgNPs have two ways of interacting with cells. Smaller AgNPs can enter the cell directly, while larger nanoparticles cannot. In either case, AgNPs continuously release Ag^+ ions that attach to cell membrane structures. This attachment causes the membrane to become unstable, leading to the leakage of protons. The destabilization of the cell wall greatly increases its permeability, which enables larger AgNPs to enter the cell.

The release of high concentrations of Ag^+ by AgNPs results in significant levels of oxidative stress, as shown in Figure 1.6. Although antioxidant enzymes play a role in removing some released ions, they are insufficient in neutralising the amount released by AgNPs. These organisms engage with proteins in the chain found on cell membranes, leading to the deactivation of enzymes. This occurs because they have an attraction to phosphate, thiol, and carboxyl groups. By binding to phosphate groups, they hinder the process of protein phosphorylation, which is often necessary for enzyme activation. Consequently, bacterial growth is inhibited [13]. AgNPs antibacterial activity differs in the cell wall structure of Gram-negative and Gram-positive bacteria [14].

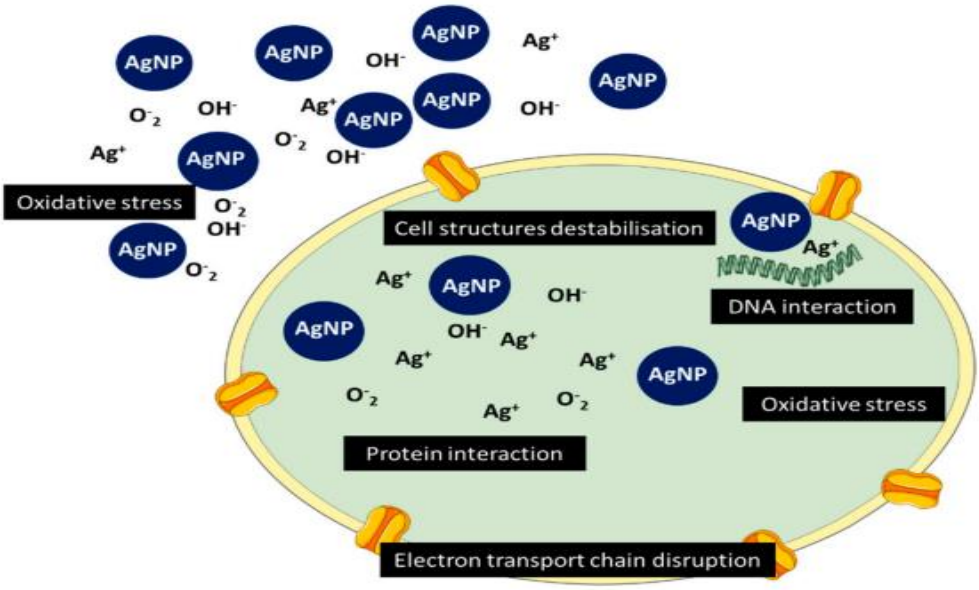

Figure 1.6: The mechanism of antimicrobial activity of AgNPs. [13]

1.4.1.3 Toxicity

The toxicity of AgNPs is relies on chemical properties, such as surface charge, solubility, shape, size, and agglomeration. Compared to bulk counterparts, AgNPs have a high surface area, making them highly reactive in environments and posing a higher risk of toxic events. Negatively charged nanoparticles are less harmful than positively charged nanoparticles additionally, AgNPs toxicity increases under acidic conditions such as those found in the stomach. The NPs shape is also a factor that affects cytotoxicity, with nanospheres presenting less toxicity when compared to with other forms. Further research is necessary to determine whether the toxicity of nanoparticles is caused by the particles themselves or the silver ions they emit. These particles are harmful to humans through various mechanisms, primarily related to their oxidative properties resulting from their interaction with thiol groups found in proteins and enzymes, which are essential components of the cell's antioxidant defence mechanisms.

AgNPs have the potential to cause DNA damage, including chromosomal aberrations due to their genotoxic properties [13].

1.4.2 Gold Nanoparticles

Gold nanoparticles (AuNPs) are clusters of particles that have a gold core. They are biocompatible and inert, which makes them safe to use. One of the advantages of AuNPs is that they can be synthesized in various sizes, shapes, and surface properties. The coating on the particles can also be modified to make them more soluble, stable, and environmentally friendly. Gold possesses valuable optical and electronic properties, which render it highly beneficial in the medical industry. Researchers have also

found that AuNPs may have antibacterial properties, which is exciting since they are less toxic to mammalian cells than the most common nanoparticles used for antimicrobial agents, AgNPs.

1.4.2.1 Synthesis

The chemical precipitation method, shown in Figure 1.7, is commonly used to synthesise gold nanoparticles. In this method, chloroauric acid (HAuCl4) undergoes a reduction reaction. Then agglomerates with the help of a stabilising agent [13].

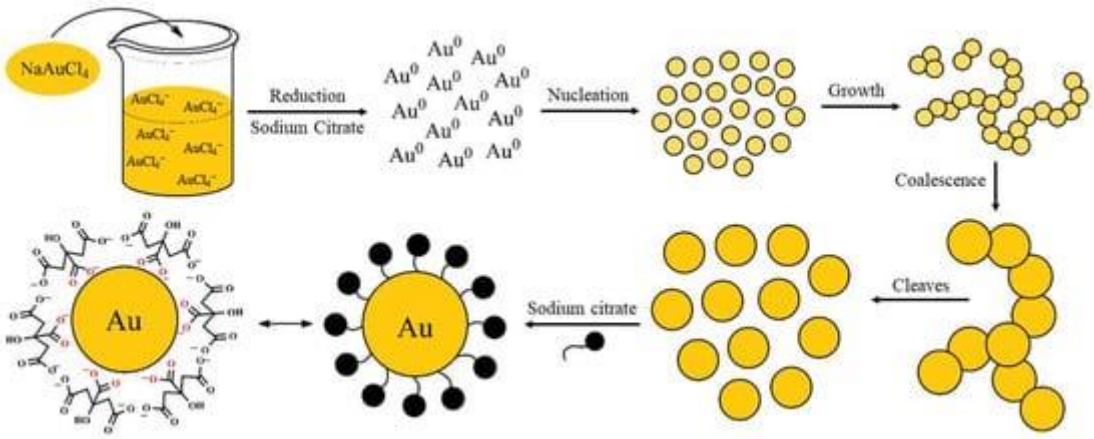

Figure1.7: Process for the synthesis of AuNPs [15].

The surface plasmon resonance of the newly formed AuNPs causes a colour change in the solution from pale yellow to pinkish red, allowing for easy detection of the reaction.

1.4.2.2 Toxicity

Despite the potential of AuNPs, their toxicity *in vitro* and *in vivo* remains uncertain due to various complex factors. These factors include dose dependence, biological interactions, and the differences between *in vitro* and *in vivo* models. Researchers conducted a study on the toxicity of AuNPs *in vitro*, indicating that these nanoparticles trigger the production of endogenous ROS upon entering the cells, which results in oxidative stress-related cytotoxicity such as DNA damage, cell death, and cell cycle arrest. For instance, in an in vitro cell viability test, gold particles sized 15-20 nm caused a drop in cell viability from 100% at a concentration of 0.1 ppm to less than 40% at 10 ppm, indicating their potential toxicity. [13].

1.4.2.3 Antimicrobial Activity

Gold nanoparticles (AuNPs) have the potential to fight against both Gram-positive, P. aeruginosa, and E. faecalis, and Gram-negative bacteria, E. coli. It is important to note that AuNPs are not naturally

antibacterial; instead, their primary method of attacking bacteria involves sticking to surfaces due to electrostatic forces. This adhesion process is influenced by the size of the nanoparticles, with smaller ones requiring Minimum Inhibitory Concentrations (MIC), the lowest concentration of a substance, in this case, AuNPs, that inhibit the growth of a microorganism, for effectiveness. Once adhered to the bacterial surfaces, AuNPs can disrupt membrane potential and hinder adenosine triphosphatase (ATPase) activity (which affects ATP synthesis). Interfere with transfer RNA (tRNA) binding in the ribosome subunit. These disruptions collectively interfere with metabolic processes. Ultimately compromise cellular integrity. When compared to other metal-based nanoparticles such as AgNPs, AuNPs are less reactive. Primarily use different mechanisms rather than ion release or reactive oxygen species (ROS) production for their antibacterial effects. As a result, higher concentrations of AuNPs are often needed to achieve efficacy as other metal-based nanoparticles.

A previous study discovered that to create an area of bacteria inhibition for S. Aureus, the use of AuNPs necessitated a concentration of 197 µg/mL. AgNPs achieved comparable effects at a significantly lower concentration of approximately 4.86 µg/mL [13].

1.4.3 Zinc Oxide Nanoparticles

Zinc is a crucial mineral found in all tissues and plays a vital role in enzyme function. It is also a biocompatible semiconductor used in various products, including as an antibacterial agent. The optical properties of ZnONPs enable them to be used in a range of therapeutic and diagnostic applications—these properties, such as photoluminescence, fluorescence, photothermal, effect, and ROS generation. When combined with appropriate functionalisation and targeting methods, they hold the potential for selective and effective antitumor therapies, antibacterial treatments, and theragnostic tools in the fight against cancer and infectious diseases [13].

1.4.3.1 Synthesis

Chemical precipitation is a common technique to synthesize ZnONPs, which was used in this project. The primary precursors to synthesize ZnONPs are zinc nitrate ($Zn(NO_3)_2$), zinc sulphate ($ZnSO_4$), and zinc acetate ($Zn(CH_3COO)_2$). Zinc oxide exists in two forms: hexagonal wurtzite, which is the most stable and prevalent, and cubic zinc blend. Additionally, when ZnONPs aggregate, they can exhibit morphologies such as nanorings or nanocages depending on the synthetic route [13]. In this study, the ZnONPs produced appeared as a white dust.

1.4.3.2 Toxicity

Despite acknowledging the benefits of ZnONPs bactericidal effects, there are lingering concerns regarding their toxicity and impact on health. Although metal-based nanoparticles are typically more harmful to bacteria than to eukaryotic cells. Their widespread presence and long-term accumulation

imply that the same mechanisms that make them effective against bacteria may also have adverse effects. The generation of oxygen species (ROS) by ZnONPs and the resulting oxidative stress have been associated with processes that could contribute to different conditions such as lung diseases and liver damage. [13].

1.4.3.3 Antimicrobial Activity

Zinc oxide nanoparticles (ZnONPs) have exhibited antibacterial properties against both Gram-positive and Gram-negative bacteria, including *S. aureus, S. epidermis, B. subtilis, B. cereus, L. monocytogenes, E. faecium, P. aeruginosa, E. coli, K. pneumoniae, and Salmonella sp*. The effectiveness of ZnONPs varies between bacterium types, with minimum inhibitory concentration (MIC) values observed in Gram-positive bacteria compared to Gram-negative by around 50-85%, being more effective against gram-positive bacteria. This difference in activity is attributed to the interactions between ZnONPs and the bacterial cell wall structure. In the case of Gram-negative bacteria, specifically, lipopolysaccharides can stop ion passage through the outer membrane hindering the attachment of ZnONPs.

These nanoparticles exert their toxicity by affecting cell membranes through different mechanisms. They alter membrane potential by blocking K^+ ion channels in these membranes. When dissolved in media, ZnONPs release Zn^{2+} ions attracted to surfaces, increasing membrane permeability while destabilizing it simultaneously. Additionally, ZnONPs generate ROS, further contributing to their effect. The positive charge of Zn^{2+} ions allow them to penetrate cell walls effectively and disrupt metabolic pathways by interacting with lipids, proteins, and nucleic acids. Zinc oxide nanoparticles (ZnONPs) have been found to have effects in acidic environments due to increased dissolution and Zn^{2+} release [13].

1.5 Antiseptics

An increasing emergence of resistance against both topical and systemic antibiotics is observed. When it comes to treating wounds, antiseptics are a better option than antibiotics because they can kill a wide range of microorganisms and have multiple ways of attacking them. This makes it less likely for bacteria to become resistant to their effects. Therefore, topical antibiotics should be discouraged if appropriate antiseptics are available. A recent World Health Organization (WHO) guideline advocates the use of good antiseptics perioperatively while reducing the use of systemic antibiotics. Generally, an ideal antiseptic should possess the following characteristics: broad-spectrum antimicrobial activity, the ability to penetrate biofilms, necrotic tissue, and eschar, low potential for acquired resistance, supportive effects on wound healing by reducing excessive inflammation, and good local tolerability. However, not all antiseptics are useful for preventing and treating infections in wound care.[15].

The antiseptics used in this project are iodine carriers such as PVP-I, and chlorine like CHX, and OCT. These three antiseptics share several characteristics, such as antimicrobial properties and topical application. They all work to kill or inhibit microorganism growth, but they do so through different

mechanisms. Chlorhexidine disrupts the cell membranes of microorganisms, octenidine disrupts the cell membranes and protein structures, and povidone-iodine releases iodine to interfere with the metabolism of microorganisms [16].

1.6 Macrophages Role in Wound Healing

Macrophages are crucial in wound healing, performing different functions to ensure proper recovery. Macrophages phenotype evolves with the stages of wound healing [17]. After an injury, proinflammatory macrophages, commonly called "M1" macrophages, enter the wound site to clean it by removing bacteria, foreign particles, and dead cells. As acute wounds heal, the macrophage population changes into a type that promotes regenerative effects, collectively known as "M2" macrophages. These M2 macrophages encourage the migration and growth of fibroblasts, keratinocytes, and endothelial cells to restore the dermis, epidermis, and blood vessels, respectively. Leading to wound closure and scar formation. Additionally, macrophages help with vascularisation by positioning themselves near forming blood vessels and assisting in stabilisation and fusion. [18]. During the remodelling phase, macrophages release enzymes called matrix metalloproteinases (MMPs) to break down the temporary extracellular matrix. These macrophages then undergo apoptosis so the skin can return to its pre-wounded state [17].

1.6.1 Importance of Macrophages

Macrophages are critical to the body's innate immune system and serve as the first defence against harmful invaders. They can be found in almost all tissues and organs and are among the first immune cells to encounter foreign particles that enter the body. Recent studies have shown that even non-toxic nanoparticles can interfere with developing the body's immune response, leading to inadequate reactions and eventual health consequences. This study examined nanoparticles' physical and chemical characteristics, such as size, shape, charge, and surface properties, to determine their impact on macrophages. To do this, researchers exposed PMA-differentiated THP-1 cells to various materials with different chemical compositions and sizes. These cells are a suitable model system for studying macrophage functions *in vitro* [19].

1.7 Main Goals of this Project

The main goal of this project was to produce and distinguish scaffolds loaded with antimicrobial agents (common antiseptics and metallic nanoparticles). This requires achieving the following step-by-step goals:

- Production of metallic nanoparticles with antimicrobial activity;

- Determination of maximum concentration of antimicrobial agents in solution that are not cytotoxic towards macrophages;
- Production and functionalisation of the scaffold's membrane with antimicrobial agents.

2 MATERIALS AND METHODS

2.1 Nanoparticles Synthesis

The method used in this project to produce the different nanoparticles was the chemical reduction method, consisting of a metal precursor dissolved in a solvent mixed with a suitable reducing agent and a surfactant in a constant stir. When there are multiple metal cationic species in the solvent, it creates a nanosized phase with varying composition. This is a promising method for producing stable metal nanoparticles. The choice of reducing agent is extensive and can be based on the specific redox thermodynamics.

2.1.1 Silver Nanoparticles Synthesis

To synthesize AgNPs by the chemical precipitation method, silver nitrate was used as the silver precursor, purchased from PanReac (CAS-7761-88-8), at a concentration of, 29.50 mM in 500 µL of water. The reducing agent was sodium borohydride, purchased from Scharlau (CAS-16940-66-2), at a concentration of 29.50 mM in 500 µL of water. As a capping agent polyvinylpyrrolidone (PVP) was used, 5.500 kDa, purchased from Aldrich (CAS-9003-39-8) at a concentration of 1% in 500 µL of water. The solutes had their mass measured using a digital scale and then dissolved in deionized water. Afterwards, the silver nitrate and the PVP solution were added to a flask, with low agitation on an ice bath. Agitation was increased before adding sodium borohydride to the solution, resulting in a coffee-coloured solution.

2.1.2 Zinc Oxide Nanoparticles Synthesis

ZnONPs were synthesized using the same method as the other particles. Zinc acetate was used as the zinc precursor, purchased from Alfa Aesar (CAS-5970-45-6), at a concentration of 0.050 M, the sodium hydroxide was used as the reducing agent, purchased from Honeywell | Fluka (CAS-1310-73-2), at a concentration of 0.25 M and the synthesis occurred at room temperature by the addition of sodium hydroxide to the zinc acetate solution. Once the precipitated was separated from the remaining solvent, deionized water at a ratio of 1:2 of zinc precursor to reducing agent, the solution had to be

centrifuged. Next precipitated was separated it was set out to dry in an oven at 50 °C for 24 hours, to evaporate the rest of the solvent. Lastly to obtain zinc oxide nanoparticles, the precipitated was sintered in a muffle for 2 hours at 200°C.

2.1.3 Gold Nanoparticles Synthesis

AuNPs like the rest of the NPs was obtained through the chemical precipitation method. The gold precursor was Gold (III) chloride solution, purchased from Sigma Aldrich (CAS-16903-35-8). Sodium borohydride was used as the reducing agent, purchased form Scharlau (CAS-16940-66-2), at a concentration of 14.75mM in 500 µL of water. As a capping agent, Polyvinylpyrrolidone (PVP) 5.500 kDa was used, purchased from Aldrich (CAS-9003-39-8) at a concentration of 1% in 500 µL of water. The solutes had their mass measured using a digital scale and then dissolved with deionized water. Afterwards, the gold chloride and the PVP solution were added to a flask, with low agitation on an ice bath, then, the agitation was increased, and the sodium borohydride was added dropwise to the solution. As a result, the obtained solution displayed a pinkish red colour.

2.2 Dynamic Light Scattering

The Dynamic Light Scattering (DLS) technique is based on the Brownian motion principle of particles in a dispersed medium. This principle states that particles are constantly moving due to collisions with solvent molecules, which transfer energy and cause particle movement. The energy transferred is constant, meaning that smaller particles move faster than larger ones. By measuring particle speed, the hydrodynamic diameter can be calculated, taking into account all influencing factors.[20]. The hydrodynamic size of the NPs was measured at room temperature using the SZ-100 nanoparticle series from Horiba Lda, with a laser of 532 nm. These measurements were performed with diluted nanoparticles, using a quartz cuvette on a scattering angle of 90° [21].

2.3 Electrospinning Procedure

Polymeric solutions were employed to produce nanofiber matrices, these solutions were produced using three different polymers Polycaprolactone (PCL), Chitosan (CHS), and Gelatine (GEL) and as solvents it was used distilled water and acetic acid. The solutions were magnetic stirred overnight at room temperature up to complete dissolution of the polymer. Also aiming to incorporate metallic nanoparticles, AuNPs, AgNPs, and ZnONPs, and antiseptics, CHX, PVP-I, and OCT. Each solution was loaded into a 5 mL syringe with a stainless-steel blunt needle attached. The needle gauge size ranged from 21 to 23 G, depending on the viscosity of the solution, causing a difference in diameter. A syringe pump (SyringePump NE-300) was used to control the flow rate. A high-voltage power supply applied voltage to the needle. An aluminium plate grounded and kept 20 cm from the needle tip was used to collect the fibres. The collector was covered with a paper foil to facilitate the detachment of the fibre mats [22]. The following tables (2.1 and 2.2) present the concentration and deposition parameters of the matrices.

Table 2.1: Polymers with antiseptics and respective deposition parameters

Polymer	Antiseptic	Weight (%)		Solvent	Deposition Parameters		
		Polymer	Antiseptic		Rate	Applied voltage	Temperature
Chitosan*	CHX	2%	2%	Ac. Acetic (90%) +H20(10%)	1.0 mL/h	16.2 kV	25-30ºC
	PVP-I	2%	2%	Ac. Acetic (90%) +H20(10%)	1.3 mL/h	18.0 kV	25-30ºC
	OCT	2%	0.1%	Ac. Acetic (90%) +H20(10%)	1.3 mL/h	17.6 kV	25-30ºC
Gelatin	CHX	25%	2%	Ac. Acetic (90%) +H20(10%)	0.3 mL/h	22.0 kV	25-30ºC
	PVP-I	25%	8%	Ac. Acetic (90%) +H20(10%)	0.3 mL/h	21.0 kV	25-30ºC
	OCT	25%	0.1%	Ac. Acetic (90%) +H20(10%)	0.3 mL/h	20.2 kV	25-30ºC
Polycaprolactone (PCL)	CHX	22%	2%	Ac. Acetic (90%) +H20(10%)	1.3 mL/h	20.9 kV	25-30ºC
	PVP-I	12%	3%	Dichloromethane	2.0 mL/h	21.0 kV	25-30ºC
	OCT	20%	0.1%	Ac. Acetic (90%) +H20(10%)	1.3 mL/h	20.5 kV	25-30ºC

* Used polyethylene oxide (PEO), to make CS suitable for electrospinning

Table 2.2: Polymers with metallic nanoparticles and respective deposition parameters

Polymer	Metallic NPs	Weight (%)	Volume (µl)	Solvent	Deposition Parameters		
		Polymer	NPs		Rate	Applied voltage	Temperature
Chitosan*	AgNPs	2%	600	Ac. Acetic (90%)	1.0 mL/h	16.24 kV	25-30ºC
	ZnONPs	2%	600	Ac. Acetic (90%)	1.3 mL/h	18 kV	25-30ºC
Gelatin	AgNPs	25%	600	Ac. Acetic (90%)	0.3 mL/h	22.0 kV	25-30ºC
	ZnONPs	25%	600	Ac. Acetic (90%)	0.3 mL/h	21.0 kV	25-30ºC
Polycaprolactone (PCL)	AgNPs	22%	600	Chloroform	1.3 mL/h	20.85 kV	25-30ºC
	ZnONPs	12%	600	Ac. Acetic (90%)	2.0 mL/h	21.0 kV	25-30ºC

2.4 Chemical Cross-Liking

To strengthen polymeric molecules and improve their properties, chemical cross-linking is often used. Glutaraldehyde, which contains carbonyl groups that can covalently bond with amino groups found in chitosan and gelatine, is a common cross-linking agent. This forms a cross-linked network that enhances mechanical strength and durability properties. The fibrous mats were placed in a plastic box with 50% glutaraldehyde (GTA) to cross-link both CS and GEL fibres. The box was closed and put in the oven at 37 ºC for 3 hours.

2.5 SEM Analysis

The Scanning Electron Microscopy (SEM) is a tool that creates a magnified image using electrons instead of light. An electron gun produces a beam of electrons through the microscope, which is held in a vacuum. As the beam goes through electromagnetic fields and lenses, it focuses down on the sample. When the beam contacts the sample, it causes the release of electrons and X-rays. Detectors gather these X-rays, backscattered electrons, and secondary electrons and convert them into a signal that goes to a screen [23]. This produces the final image, allowing for studying the morphology of fibres by using the ImageJ software to measure their diameter. The metallic nanoparticles were analysed using the Zeiss-DSM 962 Auriga electron microscope, and the fibre mats were analysed using the Hitachi tabletop microscope TM3030 Plus. Before observation, the samples were coated with Iridium using a sputter.

2.6 Cytotoxicity

NPs have been limited in their use in healthcare due to their potential toxicity, despite their antiseptic properties. This study aims to include NPs in nanofiber matrices for burn and chronic wound coverings, making it important to determine their effect on macrophages. Cell cultures were carried out to test the cell viability of nanofiber matrices with NPs, and indirect contact cytotoxicity tests were performed. The matrices were placed in vials containing complete culture medium at a con- centration of 10 mg/mL and were incubated at 37°C and 5% CO2 for 48h to produce the extracts. All procedures were performed sterile using a ESCO model labculture Sterile laminar flow chamber and sterile materials, with ethanol when talking about the fibrous mats and dry heat for the powders. Samples were tested in triplicate for reproducibility of results for NPs, antiseptics, and fibrous mats.

2.6.1 Resazurin Assay

To determine the toxicity of various nanoparticles, we first counted the number of THP-1 monocyte cells (ATCC® TIB-202TM) seeded at a density of 250,000 cells/mL in 96 well culture plates, with 25,000 cells per well and complete culture medium (RPMI 1640 supplemented with 10% heat-inactivated fetal bovine serum from Biowest, as well as 1% penicillin-streptomycin, 1% gluta- mine, 1% non-essential amino acids, and 1% sodium pyruvate from Gibco). To differentiate the mono- cytes into macrophages, it was added 8 nm PMA (from Sigma Aldrich) to the culture medium, and after 48 hours, replaced the medium with different types of nanoparticles (initial concentration of 200 ug/mL for AuNPs and AgNPs and, 50 ug/mL for ZnONPs), antiseptics (initial concentration 10 mg/mL) and fibrous mats extracts dispersed in culture medium. The five dilutions were used in a factor of two. As controls, we used cells in complete culture medium and cells in culture medium with 10% DMSO as negative and positive controls, respectively. After 48 hours of incubation at 37ºC and 5% CO2, it was used the metabolic resazurin assay to determine cell viability. Resazurin (Alfa Aesar, CAS-62758-13-8), a solution of 0.040 mg/mL in PBS, was used as a viability indicator [24]. Viable cells reduce blue and low fluorescence resazurin to pink and high fluorescence resorufin, as shown in figure 2.1. To start the final step of the procedure the suspended nanoparticles were carefully removed. Afterwards it was added new culture medium (100 µL per well) with 50% resazurin and 50% medium solution into the wells on the culture plate and control wells. The culture plate was placed in a CO2 incubator at 37 °C for 3 hours. Lastly, was used a plate reader to measure the absorbance of resazurin and resorufin at 600 and 570 nm. To obtain the cell viability we had subtract the absorption peak of resazurin at 600 nm from the absorption peak of resorufin at 570 nm. The propagation of standard deviations calculates the associated uncertainty.

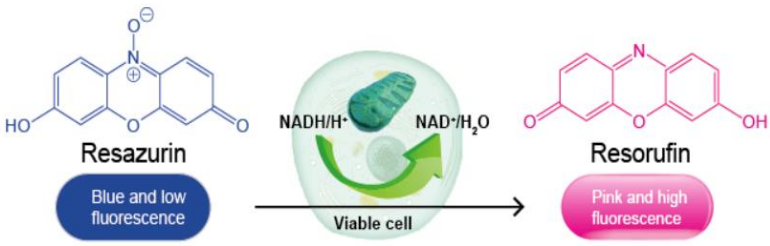

Figure 2.1: Resazurin reduction to resorufin to evaluate cell viability [26].

2.1 Antibacterial Activity

The microdilution method for estimation of minimum inhibitory concentration (MIC), determined using 96-well plates, was used to quantify metallic nanoparticles antibacterial activity against E.coli, ATCC DH3alfa. Briefly, MICs were determined by incubating the organisms in 96-well microplates for 18-24 hours at 37ºC under aerobic conditions for all bacterial strains. Microorganisms were exposed to serial dilutions of NPs ranging from 25 to 200 µg/mL and the endpoints were determined when no turbidity in the well was observed, no turbidity meant no growth. If there was turbidity it meant there were bac- terial growth. Thus, 10µl of each clear culture was spotted on trypticase soy broth (TSB) for evaluating the minimum bacterial concentration (MBC). All assays were performed triplicate.

3 RESULTS AND DISCUSSION

3.1 Nanoparticle Analysis

3.1.1 DLS

The size of the nanoparticles was determined using the DLS technique. The chemical precipitation method was used to synthesise the nanoparticles, which affects their size and shape. According to Table 3.1, the average hydrodynamic size and PDI (Polydispersity Index) for AgNPs was 60±4 nm and 0.2, respectively. A PDI value of 0 indicates a monodisperse distribution. Values smaller than 0.05 are seen in highly monodisperse standards, while values above 0.7 indicate a broad particle size and are not suitable for analysis by the DLS technique [25]. The PDI value obtained of 0.2 for the AgNPs is acceptable, meaning they are highly monodispersing, but there is still room for improvement.

The average size of AuNPs was <10 nm, and the PDI was 0.18 ±0.03. Gold nanoparticles are smaller particles when compared with the other particles. According to references, particles smaller than 10 nm can be categorized as ultrasmall. As shown in Table 3.1, the obtained AuNPs were ultrasmall particles with an average size <10 nm, and the PDI was 0.18 ±0.03, indicating a narrow and uniform size distribution. The particles within the sample are consistent and closely clustered around the average size. In contrast, ZnONPs were much bigger, measuring 195±26 nm, possibly due to the presence of aggregates. According to the literature, aggregation may be caused by a decrease in stability leading to a rise in the surface charge. The obtained PDI for ZnONPs was 0.12±0.05, indicating a uniform size distribution. Researchers obtained a PDI of 0.206 for ZnONPs, indicating a high monodispersity of the nanoparticles. Values around 0.1 are considered good or uniform for a monomodal dispersion [26].

Table 3.1: Metallic Nanoparticles measurements from DLS

Sample	Dh1 (nm)	Dh2 (nm)	Polydispersity index
ZnONPs	195±26	-	0.12±0.05
AgNPs	7±1	60±4	0.21±0.10
AuNPs	<10 nm	-	0.18±0.03

3.1.2 SEM

SEM was used to determine the diameter of the metallic nanoparticles produced by the chemical precipitation method. Subsequently, the Image J software was used to determine the diameter of at least 20 particles at a magnification of 5000x, at higher magnifications SEM loses resolution. Figure 3.1 shows the SEM images of ZnONPs and AgNPs.

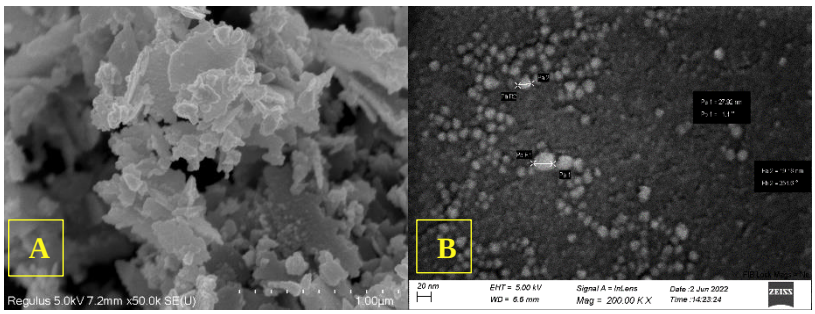

Figure 3.1: (A) Zinc Oxide (0,050mM) and (B)Silver Nanoparticles (29,50 mM) produced by chemical precipitation method on image using SEM

According to figure 3.1 (A) ZnONPs morphology is some sort of triangular flakes, being very different from the ones in the literature, for example the most stable ZnONPs have a hexagonal wurtzite form. According to table 3.2 ZnONPs average diameter was 195 nm, value when compared to the DLS value from table 3.1 for ZnONPs we can see that the values match. This means that the size distribution of the NPs is relatively monodisperse. AgNPs (B) show a spherical shape which was the desired form for these particles. AgNPs diameter shown in table 3.2 is of 9.1 nm. This size is contained in the 7 nm to 61 nm range obtained by DLS.

Table 3.2: Average fibre diameter of ZnONPs and AgNPs obtained from SEM

Sample	Mean (SEM) (nm)	Standard deviation (nm)
ZnONPs	195	151
AgNPs	9.1	2.5

3.2 Nanofiber morphology analysis

The fibrous mats from PCL, CS and GEL loaded with metallic nanoparticles or antiseptics were obtained using ES technique for antimicrobial wound dressings. To measure the diameter of polymeric electrospun fibers and assess their morphology, it was used Scanning Electron Microscopy (SEM). For each fibrous mat, at least 20 fibers were examined at a 5000x magnification and used Image J processing software to accurately determine their average diameter.

3.2.1 SEM: Polycaprolactone (PCL)

Figure 3.2 shows SEM of PCL fibres loaded with either antiseptics or metallic nanoparticles.

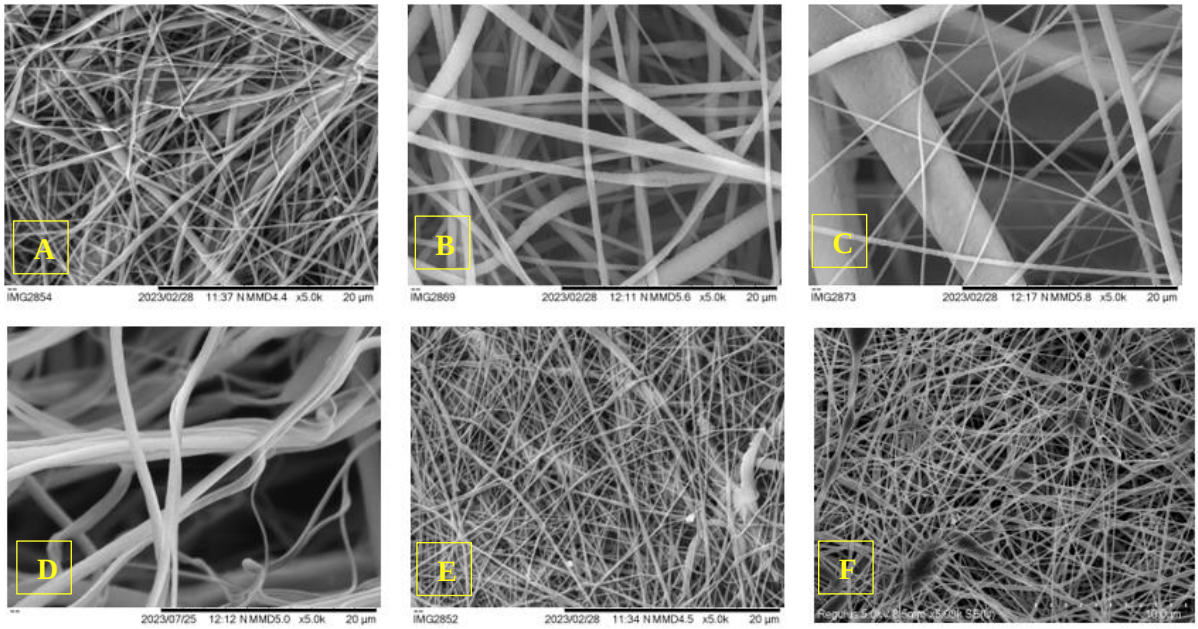

Figure 3.2: SEM images of PCL electrospun mats at a scale of 20 µm produced from: (A)PCL, (B)PCL+AgNPs, (C)PCL+ZnONPs, (D)PCL+PVP-I, (E)PCL+CHX, (F)PCL+OCT.

The SEM micrographs above depict pure PCL (image 3.2-A) and two fibrous mats of PCL+OCT and PCL+CHX beads that displays non-uniform fibres of varying diameters and no beads. Image B, AgNPs, shows a smaller diameter than pure PCL and ZnONPs, image C, since AgNPs make the PCL solution more conductive when loaded, ultimately leading to a decrease in diameter that might have been caused by rapid evaporation or higher viscosity. PCL+ZnONPs show an increase in diameter when compared to pure PCL, it is free of beads and non-uniform. Image 3.2D, PCL+PVP-I, displays a significant dispersion between diameters, with fiber diameter being affected by PVP-I viscosity. According to literature the addition of PVP-I to the solution increases it viscosity causing the fibers to be thicker and so having a bigger diameter [27].

PCL+OCT fibrous mats form beads due to the low concentration of OCT used (0.1%), as stated in the article [28]. PCL fibres incorporated with OCT did not form beads when the loading of OCT was above 5%.

Table 3.3 presents the average diameter of PCL electrospun mats. Compared to pure PCL, the average fibre diameter increases for PCL+AgNPs, and decreases for PCL+OCT, and PCL+CHX, while it increases in PCL+PVP-I.

Table 3.3: Average fibre diameter of PCL matrices obtained from SEM

Sample	Mean (SEM) (nm)	Standard deviation (nm)
PCL	375	210
PCL+AgNPs	1031	583
PCL+ZnONPs	957	1610
PCL+OCT	180	77
PCL+PVP-I	804	296
PCL+CHX	239	70

3.2.2 SEM: Gelatine (GEL)

The following image 3.3 shows samples of the polymer GEL and its mixtures with the antiseptics and the metallic nanoparticles.

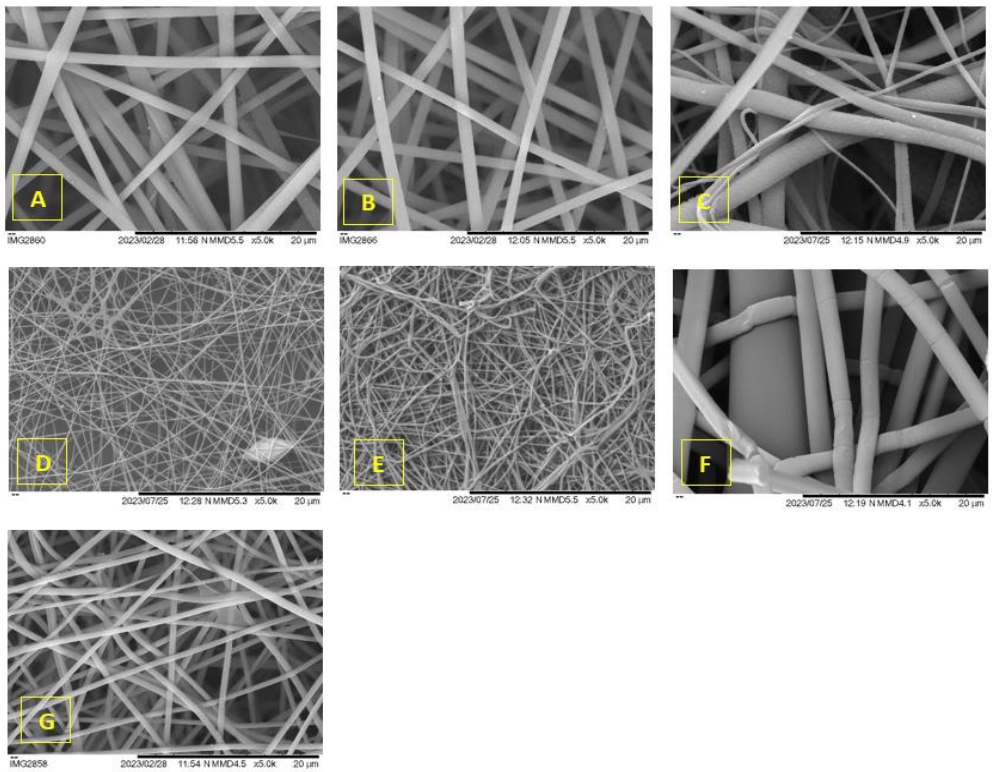

Figure 3.3: SEM images of GEL electrospun mats produced from: (A)GEL before crossliking, (B)GEL after crosslinking, (C)GEL+AgNPs, (D)GEL+OCT, (E)GEL+CHX, (F)GEL+PVP-I, (G) GEL+ZnONPs (All the other mats were cross-linked with GTA)

Cross-linked and not cross-linked GEL (B and A, respectively) present themselves as being regular, with no defects with similar average diameters, which means that cross-linking affects neither the diameter of the fibers nor their morphology.

According to figure 3.3, beads are formed in GEL loaded with OCT mats, similar to what happened with PCL loaded with OCT. Even though one is cross-linked and the other isn't there are no visible differences between the two. When GEL is loaded with AgNPs the fibers diameter decreases slightly but the standard deviation, increases significantly, as it happened in PCL loaded with the same particles.

When loaded with OCT there are no beads. Different from what happened when PCL is loaded with OCT even though the concentration used was the same (0,1%). According to the literature this might have happened due to decreased surface tension [29]. Which may have resulted of adding OCT to the pure GEL solution [30].

GEL fibres loaded with PVP-I, which show a significant increase in diameter, like what happened to PCL when loaded with PVP-I.

Table 3.4: Average fibre diameter of GEL matrices obtained from SEM

Sample	Mean (SEM) (nm)	Standard deviation (nm)
GEL NC *	1256	223
GEL C -	1231	178
GEL+AgNPs	1165	734
GEL+ZnONPs	190	32
GEL+CHX	235	39
GEL+PVP-I	2185	443
GEL+OCT	686	138

*NC- not cross-linked -C- Cross-linked

3.2.3 SEM: Chitosan (CS)

The following image 3.4 show samples of fibres CS and CS mixtures with the antiseptics and the metallic nanoparticles. Figure 3.4 shows that despite the morphology of the fibres mats does not change between cross-linked and not cross-linked, the diameter according to table 3.5 shows that when compared there is a decrease of diameter from not cross-linked CS to cross-linked CS. According to [31] this may be caused by the cross-linking process changing the polymer chains and density of the network structure. Comparing pure CS with the ones loaded with antiseptic or metallic nanoparticles there is no morphological alterations, they are all non-uniform and randomly orientated.

CS loaded with ZnONPs shows formation of beads, differently from other mats. There is no clear reason according to the literature to why this happens, it might be due to the properties of ZnONPs-CS polymer solution, viscosity and surface tension, and size, and concentration of ZnONPs and their interactions.

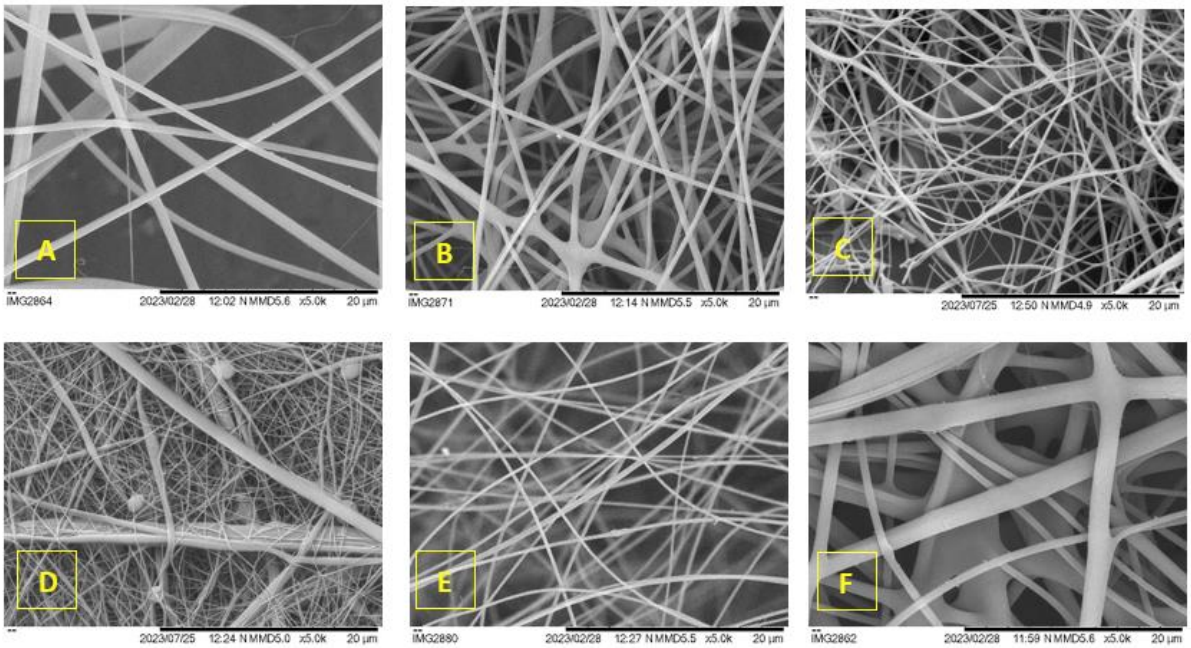

Figure 3.2: SEM images of CS electrospun mats produced from: (A)CS before crosslinking, (B)CS after cross-linking, (C)CS+AgNPs, (D)CS+ZnONPs, (E)CS+OCT, (F)CS+CHX

Table 3.5: Average fibre diameter of CS matrices obtained from SEM

Sample	Mean (SEM) (nm)	Standard deviation (nm)
CS NC*	1118	792
CS C-	656	235
CS+AgNPs	385	197
CS+ZnONPs	283	266
CS+OCT	393	74
CS+CHX	1247	549

*NC - not cross-linked -C cross-linked

3.3 Cytotoxicity

3.3.1 Metallic Nanoparticles

In figure 3.5 is presented the results for the cytotoxicity of three types of metallic nanoparticles (AgNPs, ZnONPs, and AuNPs) towards macrophages. Macrophages play a pivotal role as a first-line defence mechanism against systemically distributed nanoparticles thus they are of high relevance as model system. These cells were exposed for 48 h to different concentrations of metallic nanoparticles.

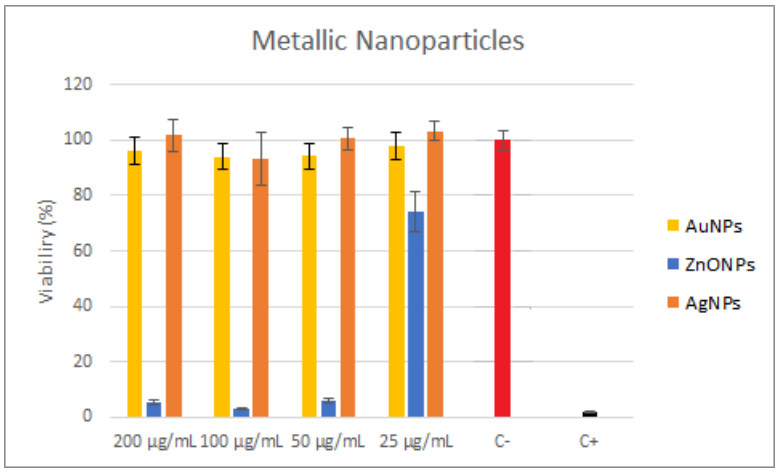

Figure 3.3: Results of differentiated THP-1 cell's viability, obtained in cytotoxic test of metallic nanoparticles

Figure 3.5 shows that the cytotoxicity of ZnONPs is dependent on doses. At concentration above 25 µg/mL, ZnONPs demonstrated higher toxicity towards macrophages. At 25 µg/mL, ZnONPs exhibited slight toxicity to cells (74% cell viability) compared to the negative control (100% cell viability). Concentrations of ZnONPs below 12.5 µg/mL indicated cell viability levels similar to the negative control at 100%. According to [32] research has also shown that ZnO-NPs presented better cell viability at lower concentrations due to the dose (time and concentration) effect on cell viability. Therefore, it can be concluded that both time and concentration affect cell viability.

Concerning AgNPs and AuNPs, cellular viability remained at around 100% for all concentrations of 200 µg/mL and below. According to literature, AgNPs cytotoxicity depends on several factors such as concentration, size, exposure time, and environmental factors. A study has shown that AuNPs with a size of 15–20 nm decrease cell viability from 100% at a concentration of 0.1 ppm to less than 40% at 10 ppm, showing their potential toxicity. *In vitro* tests have shown that AgNPs are highly toxic at 5 to 100 µg/mL concentrations and sizes from 10 to 100 nm [33]. The particle size is a significant factor for the cytotoxic nature of AgNPs since it affects the surface area-to-volume ratio and surface reactivity of nanoparticles. Previous research synthesized 15 nm and 55 nm hydrocarbon coated AgNPs and observed that the generation of ROS is higher for 15 nm compared to 55 nm AgNPs delivered to macrophage lines [34]. Therefore, it can be stated that as the particle size decreases, the cytotoxicity increases. Additionally, the morphology of NPs also affects cytotoxicity. For example, spherical nanoparticles are more subject to endocytosis than nanotubes or sharp particles.

3.3.2 Antiseptics

Figure 3.6 shows the cytotoxicity results of the three antiseptics (PVP-I, CHX, and OCT) used in this study towards macrophages.

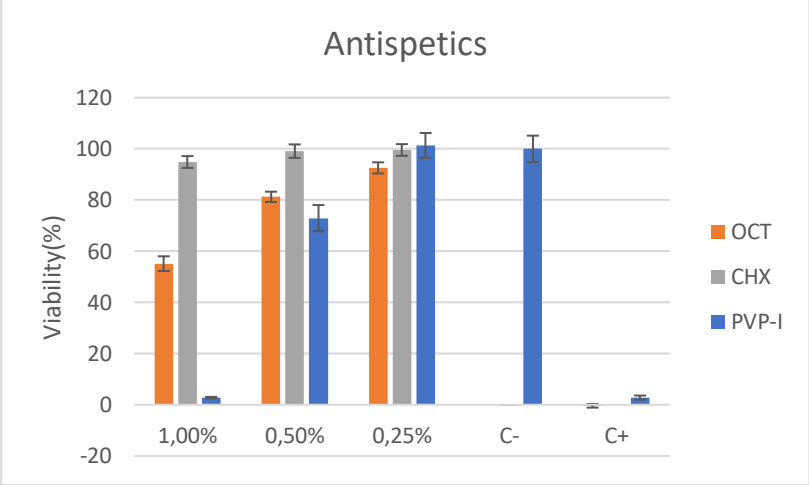

Figure 3.6: Results of differentiated THP-1 cell's viability, obtained in cytotoxic test of Antiseptics

Based on figure 3.6, it was observed that the toxicity of PVP-I is dependent on the dosage. This indicates that PVP-I is more toxic at higher concentrations and less toxic at lower ones. At a concentration of 1,00%, PVP-I was found to be highly toxic to macrophages. At a concentration of 0.5%, PVP-I showed some cell toxicity with a cell viability of 72% compared to the negative control (100% cell viability). However, for concentrations below 0.25%, PVP-I can be safely used as its cell viability is similar to the negative control, which is close to 100%.

A study conducted by [35] on PVP-I cytotoxicity towards HMEC-1 (human endothelial-like cell isolated from the endothelial cells) revealed that PVP-I is only safe below a concentration of 0.1% wt/vol. Beyond this threshold, PVP-I can kill human cells and potentially harm exposed tissues.

Similarly, OCT also showed dose-dependency in terms of toxicity. At lower concentration of 0.25%, it has a cell viability of approximately 100% and can be used safely. Lastly, CHX is the antiseptic with the most consistent viability, which is close to 100% for any of the concentrations. However, according to [24], the clinically used concentration of CHX is 2%

3.3.3 Polymeric Mats

3.3.3.1 Polycaprolactone (PCL)

In figure 3.7 are presented the results for the cytotoxicity of the polymer PCL pure and loaded with both metallic nanoparticles (AgNPs, ZnONPs, and AuNps) and antiseptics (CHX, OCT, and PVP-I) towards macrophages.

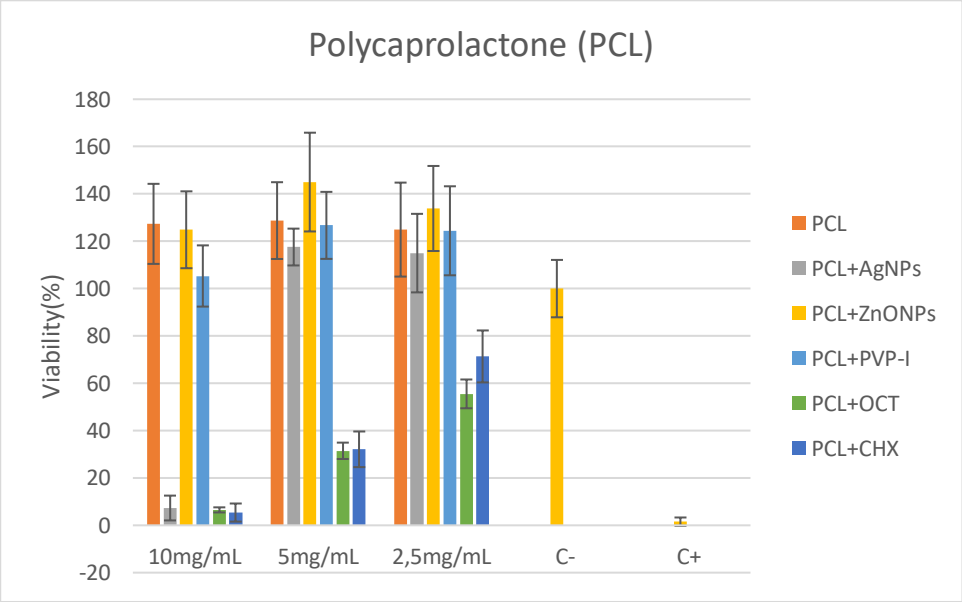

Figure 3.7: Results of differentiated THP-1 cell's viability, obtained in cytotoxic test of pure PCL and PCL loaded with metallic NPs and antiseptics

Figure 3.7 displays the resazurin assay results for cells exposed to the extracts. Pure PCL electrospun mats exhibited values around 100%, similar to the negative control, indicating no cytotoxicity. However, when antiseptics were added to the PCL solution, the resulting fibres were cytotoxic due to antiseptic release into the culture medium during extract preparation. For fibres loaded with ZnONPs, no cytotoxicity was observed for all tested concentrations, which could be due to the low quantity of ZnONPs in the fibres or their entrapment in the fibrous mats, which prevented their release into the culture media during extract preparation. PCL fibres loaded with AgNPs were toxic at a concentration

of 10 mg/mL, likely due to a high amount of AgNPs in the fibres that were easily released into the culture medium during extract preparation.

3.3.3.2 Chitosan (CS)

The cytotoxicity assay of pure CS and CS with metallic NPs and antiseptics towards THP-1 monocytic cells is shown in Figure 3.8.

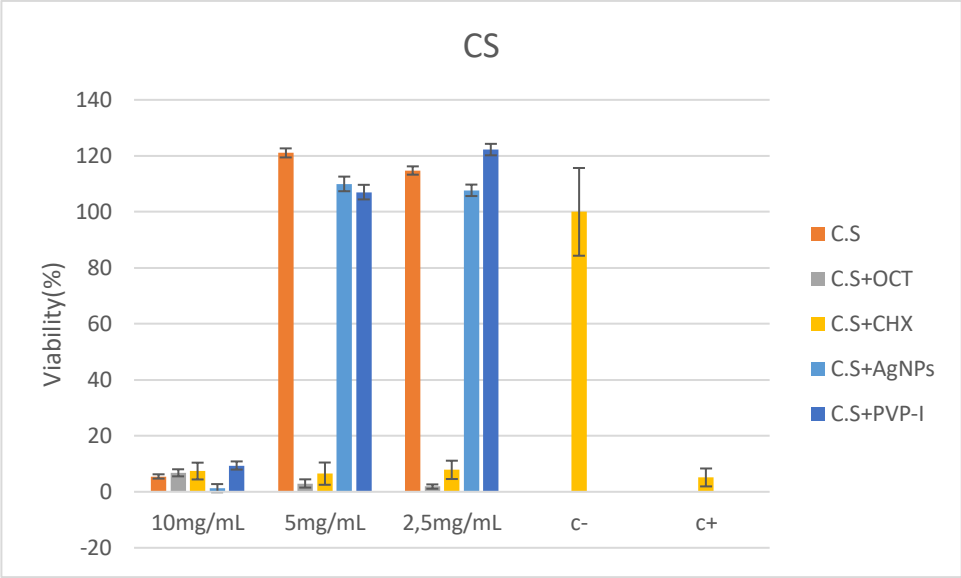

Figure 3.8: Results of differentiated THP-1 cell's viability, obtained in cytotoxic test of pure CS and CS loaded with metallic NPs and antiseptics

CS is combined with 50% GTA vapor to become cross-linked trough the reaction of carbonyl groups with the amino groups of CS to form covalent bonds. However, it may happen that some GTA remains unreacted and this GTA was not neutralized. Consequently, even though CS itself isn't toxic, when the concentration of pure CS, CS loaded with NPs, and CS loaded with antiseptics was at 10mg/mL, cell viability was close to 0% - like the positive control (which also had a cell viability of around 0%). However, for concentrations of 5 and 2.5 mg/mL, a significant increase in cell viability was seen for pure CS and CS loaded with AgNPs and PVP-I, viability values were similar to 100% compared to the control (100% cell viability), indicating the absence of cytotoxicity. However, for CS loaded with OCT and CHX, viability closer to the positive control (cell viability 0%) was observed for the same concentrations, indicating cytotoxicity of the extracts.

3.3.3.3 Gelatine (GEL)

Similarly, to the polymers mentioned above, GEL cytotoxicity was evaluated

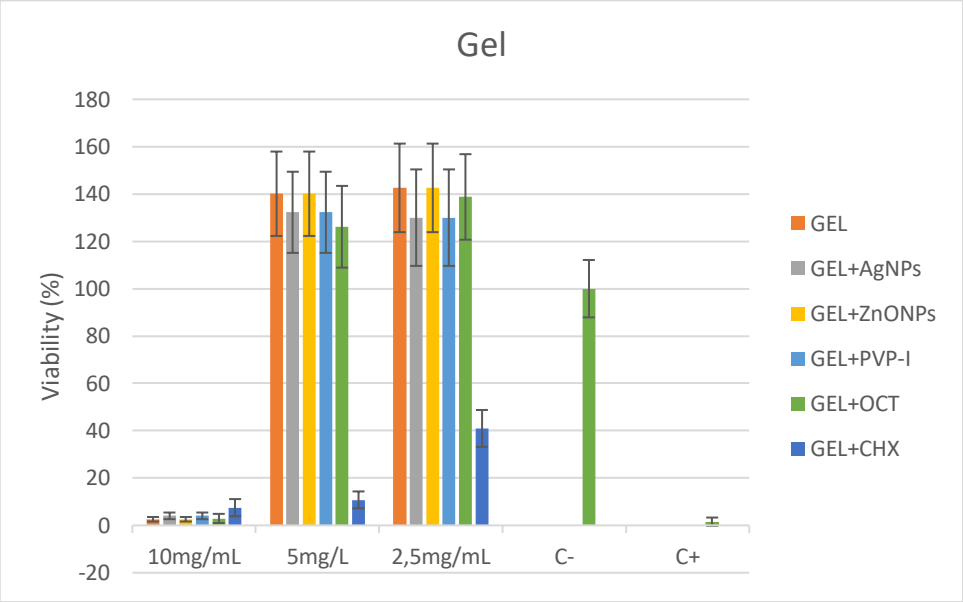

Figure 3.9: Results of differentiated THP-1 cell's viability, obtained in cytotoxic test of pure GEL and GEL loaded with metallic NPs and antiseptics

Figure 3.9 shows that, like CS, GEL, which was cross-linked with 50% GTA at higher concentrations (10mg/mL) leads to cell viability close to 0% (C+), making it toxic.

For the remaining concentrations, 5 and 2.5 mg/mL, there was a positive increase in cell viability, even surpassing 100%, as is the case for the GEL loaded with the NPs (silver and zinc) and for two of the three antiseptics, OCT, and PVP-I. Regarding the cell viability of the GEL loaded with CHX, although this increased at lower concentrations, meaning it is dose-dependent, it was still well below 100 % (approximately 40 %).

3.4 Antibacterial Activity

3.4.1 Minimum Inhibitory Concentration (MIC)

In order to determine how effective the antimicrobial agents studied in this work are against *E.coli*, gram-negative bacteria, which is one of the most common bacterial species that cause human infections, a test called the minimum inhibitory concentration (MIC) was conducted. The MIC test measures the lowest concentration of a substance that can stop visible growth of microorganisms after a 24-hour culture. To conduct the test, tryptic soy broth (TSB) growth medium was used, which has high levels of amino acids, small peptides, salts, trace minerals, and vitamins. The components of TSB can impact the surface chemistry of NPs by altering their zeta potential, dissolving them, or blocking interactions.

.

Table 3.6: MIC and MBC concentration values for *E.Coli*

E. Coli	MIC (µg/mL)			MBC (µg/mL)		
NPs	REP1	REP2	REP3	REP1	REP2	REP3
AgNPs	100	100	200	100	200	-
AuNPs	200	200	200	200	200	-
ZnONPs	50	50	50	-	50	-

After analysing the data from Table 3.6, the effectiveness of AuNPs, AgNPs, and ZnONPs in combating *E. coli* bacteria was evaluated. The results indicated that AgNPs had a minimum inhibitory concentration (MIC) of 100 µg/mL in the first two trials, which was lower compared to the third trial, where 200 µg/mL was required to achieve the same effect. The two replicas had different MBC values, with replica 1 having 100 µg/mL and the other having 200 µg/mL. Studies have shown that AgNPs obtained through green synthesis methods have lower MIC and MBC values than other methods. For instance, a study showed that Gmelina arborea-mediated AgNPs (GA-AgNPs) against *E. coli* had values of 20 µg/mL of MIC and 40 µg/mL of MBC. In comparison, the values obtained from the obtained AgNPs were less effective, requiring higher concentration to exhibit antibacterial activity [36]. AgNPs are typically more effective against gram-negative bacteria, *E.coli*, because they have a thick lipopoly-saccharide (LPS) layer in their cell wall with a thin peptidoglycan layer, making it easier for AgNPs to penetrate the bacteria.

AuNPs had MIC and MBC values of 200 µg/mL for the two replicas, with the third replica showing no antibacterial effect against *E.coli*, resulting in bacterial growth. According to a study, the antibacterial activity of AuNPs against *E.coli* was higher at 100 µg/mL than at 200 µg/mL, as shown by MIC [37]. Finally, ZnONPs exhibited a MIC value of 50 µg/mL, significantly lower than the other NPs tested, indicating that this concentration effectively inhibits *E. coli* growth. However, MIC values were more variable, with two replicas showing no effect on *E. coli* and the second replica showing inhibition of bacterial growth.

4 CONCLUSION AND FUTURE PERSPECTIVES

This thesis thoroughly examines nanoparticles, polymer-based materials, and antiseptics and how they interact. The insights gained from this research have significant potential for biomedical science, antimicrobial applications, and the advancement of biomaterials.

Among the nanoparticles studied, gold nanoparticles (AuNPs) are particularly noteworthy due to their exceptional uniformity, making them ideal for applications requiring precise control over particle size. Similarly, zinc oxide nanoparticles (ZnONPs) exhibit consistent size distribution, while silver nanoparticles (AgNPs) are slightly less uniform but still suitable for various applications.

Using scanning electron microscopy (SEM) and dynamic light scattering (DLS), the research has uncovered how additives can affect the fibre morphology within polycaprolactone (PCL) and gelatine (GEL) mats, with some additives generating finer fibres and others producing a broader distribution of fibre diameters. These findings highlight the importance of material composition in tailoring fibre characteristics and designing advanced biomaterials.

On the other hand, chitosan (CS) mats showed a significant reduction in fibre diameter through cross-linking without compromising the mat's structural integrity. Moreover, additives introduced into CS matrices did not substantially change fibre morphology, emphasizing the adaptability of CS-based materials.

According to the cytotoxicity test, ZnONPs were less harmful to cells when used in concentrations below 12.5 µg/mL. At these lower concentrations, cell viability was similar to the negative control. However, when used at higher concentrations, ZnONPs became toxic to macrophages. On the other hand, AgNPs showed minimal toxicity, with cell viability remaining at or near 100% even for concentrations up to 200 µg/mL. Meanwhile, AuNPs were highly biocompatible, with cell viability maintained at or above 100% across all tested concentrations.

Finally, the investigation into the antibacterial properties of AgNPs, AuNPs, and ZnONPs against *Escherichia coli (E. coli)* demonstrated their potential in combating bacterial infections, with ZnONPs being particularly effective at lower concentrations.

To improve the cytotoxicity, antibacterial activity, morphology, and size of the particles even though they show promising results, exploring alternative synthesis methods in future research would be beneficial. Although this study only evaluated the antibacterial activity against gram-negative bacteria, it would be worthwhile to investigate its effects on gram-positive bacteria. Silver nanoparticles, for example, exhibit distinct behaviours between the two types of bacteria.

BIBLIOGRAPHY

[1] M. Rodrigues, N. Kosaric, C. A. Bonham, e G. C. Gurtner, «Wound Healing: A Cellular Perspective», *Physiol. Rev.*, vol. 99, n.º 1, pp. 665–706, jan. 2019, doi: 10.1152/physrev.00067.2017.

[2] R. G. Frykberg e J. Banks, «Challenges in the Treatment of Chronic Wounds», *Adv. Wound Care*, vol. 4, n.º 9, pp. 560–582, set. 2015, doi: 10.1089/wound.2015.0635.

[3] P. Kolimi, S. Narala, D. Nyavanandi, A. A. A. Youssef, e N. Dudhipala, «Innovative Treatment Strategies to Accelerate Wound Healing: Trajectory and Recent Advancements», *Cells*, vol. 11, n.º 15, p. 2439, ago. 2022, doi: 10.3390/cells11152439.

[4] B. R. Freedman, C. Hwang, S. Talbot, B. Hibler, S. Matoori, e D. J. Mooney, «Breakthrough treatments for accelerated wound healing», *Sci. Adv.*, vol. 9, n.º 20, p. eade7007, mai. 2023, doi: 10.1126/sciadv.ade7007.

[5] A. Kushwaha, L. Goswami, e B. S. Kim, «Nanomaterial-Based Therapy for Wound Healing», *Nanomaterials*, vol. 12, n.º 4, p. 618, fev. 2022, doi: 10.3390/nano12040618.

[6] «Polymer-based biomaterials for pharmaceutical and biomedical applications: A focus on topical drug administration - ScienceDirect». Acedido: 29 de setembro de 2023. [Em linha]. Disponível em: https://www.sciencedirect.com/science/article/pii/S0014305723000514?via%3Dihub

[7] E. Y. Teo *et al.*, «Polycaprolactone-based fused deposition modeled mesh for delivery of antibacterial agents to infected wounds», *Biomaterials*, vol. 32, n.º 1, pp. 279–287, jan. 2011, doi: 10.1016/j.biomaterials.2010.08.089.

[8] A. Guarnieri *et al.*, «Antimicrobial properties of chitosan from different developmental stages of the bioconverter insect Hermetia illucens», *Sci. Rep.*, vol. 12, n.º 1, Art. n.º 1, mai. 2022, doi: 10.1038/s41598-022-12150-3.

[9] I. Lukin *et al.*, «Progress in Gelatin as Biomaterial for Tissue Engineering», *Pharmaceutics*, vol. 14, n.º 6, p. 1177, mai. 2022, doi: 10.3390/pharmaceutics14061177.

[10] J. Xue, T. Wu, Y. Dai, e Y. Xia, «Electrospinning and Electrospun Nanofibers: Methods, Materials, and Applications», *Chem. Rev.*, vol. 119, n.º 8, pp. 5298–5415, abr. 2019, doi: 10.1021/acs.chemrev.8b00593.

[11] A. R. Alharbi, I. M. Alarifi, W. S. Khan, e R. Asmatulu, «Highly Hydrophilic Electrospun Polyacrylonitrile/ Polyvinypyrro-lidone Nanofibers Incorporated with Gentamicin as Filter Medium for Dam Water and Wastewater Treatment», *J. Membr. Sep. Technol.*, vol. 5, n.º 2, Art. n.º 2, jul. 2016, doi: 10.6000/1929-6037.2016.05.02.1.

[12] M. Wang, S. K. Marepally, P. K. Vemula, e C. Xu, «Chapter 5 - Inorganic Nanoparticles for Transdermal Drug Delivery and Topical Application», em *Nanoscience in Dermatology*, M. R. Hamblin, P. Avci, e T. W. Prow, Eds., Boston: Academic Press, 2016, pp. 57–72. doi: 10.1016/B978-0-12-802926-8.00005-7.

[13] E. Sánchez-López *et al.*, «Metal-Based Nanoparticles as Antimicrobial Agents: An Overview», *Nanomater. Basel Switz.*, vol. 10, n.º 2, p. 292, fev. 2020, doi: 10.3390/nano10020292.

[14] P. R. More, S. Pandit, A. D. Filippis, G. Franci, I. Mijakovic, e M. Galdiero, «Silver Nanoparticles: Bactericidal and Mechanistic Approach against Drug Resistant Pathogens», *Microorganisms*, vol. 11, n.º 2, p. 369, fev. 2023, doi: 10.3390/microorganisms11020369.

[15] C. D. Roberts, D. J. Leaper, e O. Assadian, «The Role of Topical Antiseptic Agents Within Antimicrobial Stewardship Strategies for Prevention and Treatment of Surgical Site and Chronic Open Wound Infection», *Adv. Wound Care*, vol. 6, n.º 2, pp. 63–71, fev. 2017, doi: 10.1089/wound.2016.0701.

[16] P. J. Alves, R. T. Barreto, B. M. Barrois, L. G. Gryson, S. Meaume, e S. J. Monstrey, «Update on the role of antiseptics in the management of chronic wounds with critical colonisation and/or biofilm», *Int. Wound J.*, vol. 18, n.º 3, pp. 342–358, dez. 2020, doi: 10.1111/iwj.13537.

[17] P. Krzyszczyk, R. Schloss, A. Palmer, e F. Berthiaume, «The Role of Macrophages in Acute and Chronic Wound Healing and Interventions to Promote Pro-wound Healing Phenotypes», *Front. Physiol.*, vol. 9, p. 419, mai. 2018, doi: 10.3389/fphys.2018.00419.

[18] H. Hong e X. Y. Tian, «The Role of Macrophages in Vascular Repair and Regeneration after Ischemic Injury», *Int. J. Mol. Sci.*, vol. 21, n.º 17, p. 6328, ago. 2020, doi: 10.3390/ijms21176328.
[19] T. Brzicova *et al.*, «Molecular Responses in THP-1 Macrophage-Like Cells Exposed to Diverse Nanoparticles», *Nanomaterials*, vol. 9, n.º 5, Art. n.º 5, mai. 2019, doi: 10.3390/nano9050687.
[20] J. Stetefeld, S. A. McKenna, e T. R. Patel, «Dynamic light scattering: a practical guide and applications in biomedical sciences», *Biophys. Rev.*, vol. 8, n.º 4, pp. 409–427, out. 2016, doi: 10.1007/s12551-016-0218-6.
[21] P. I. P. Soares *et al.*, «Iron oxide nanoparticles stabilized with a bilayer of oleic acid for magnetic hyperthermia and MRI applications», *Appl. Surf. Sci.*, vol. 383, pp. 240–247, out. 2016, doi: 10.1016/j.apsusc.2016.04.181.
[22] «Electrospun biodegradable chitosan based-poly(urethane urea) scaffolds for soft tissue engineering», *Mater. Sci. Eng. C*, vol. 103, p. 109819, out. 2019, doi: 10.1016/j.msec.2019.109819.
[23] D. Herres, «Difference between the scanning electron microscope and scanning tunneling microscope», Design World. Acedido: 29 de setembro de 2023. [Em linha]. Disponível em: http://www.testandmeasurementtips.com/new-articles/basics-of-the-scanning-electron-microscope/
[24] J. X. Liu, J. Werner, T. Kirsch, J. D. Zuckerman, e M. S. Virk, «Cytotoxicity evaluation of chlorhexidine gluconate on human fibroblasts, myoblasts, and osteoblasts», *J. Bone Jt. Infect.*, vol. 3, n.º 4, pp. 165–172, ago. 2018, doi: 10.7150/jbji.26355.
[25] S. Khorrami, A. Zarrabi, M. Khaleghi, M. Danaei, e M. Mozafari, «Selective cytotoxicity of green synthesized silver nanoparticles against the MCF-7 tumor cell line and their enhanced antioxidant and antimicrobial properties», *Int. J. Nanomedicine*, vol. 13, pp. 8013–8024, nov. 2018, doi: 10.2147/IJN.S189295.
[26] K. N. Clayton, J. W. Salameh, S. T. Wereley, e T. L. Kinzer-Ursem, «Physical characterization of nanoparticle size and surface modification using particle scattering diffusometry», *Biomicrofluidics*, vol. 10, n.º 5, p. 054107, set. 2016, doi: 10.1063/1.4962992.
[27] H. D. López-Calderón *et al.*, «Electrospun Polyvinylpyrrolidone-Gelatin and Cellulose Acetate Bi-Layer Scaffold Loaded with Gentamicin as Possible Wound Dressing», *Polymers*, vol. 12, n.º 10, p. 2311, out. 2020, doi: 10.3390/polym12102311.
[28] M. J. Mochane, T. S. Motsoeneng, E. R. Sadiku, T. C. Mokhena, e J. S. Sefadi, «Morphology and Properties of Electrospun PCL and Its Composites for Medical Applications: A Mini Review», *Appl. Sci.*, vol. 9, n.º 11, Art. n.º 11, jan. 2019, doi: 10.3390/app9112205.
[29] H. R. El-Seedi *et al.*, «Gelatin nanofibers: Recent insights in synthesis, bio-medical applications and limitations», *Heliyon*, vol. 9, n.º 5, p. e16228, mai. 2023, doi: 10.1016/j.heliyon.2023.e16228.
[30] N. Amariei, L. R. Manea, A. P. Bertea, A. Bertea, e A. Popa, «The Influence of Polymer Solution on the Properties of Electrospun 3D Nanostructures», *IOP Conf. Ser. Mater. Sci. Eng.*, vol. 209, n.º 1, p. 012092, jun. 2017, doi: 10.1088/1757-899X/209/1/012092.
[31] H. Niknejad e R. Mahmoudzadeh, «Comparison of Different Crosslinking Methods for Preparation of Docetaxel-loaded Albumin Nanoparticles», *Iran. J. Pharm. Res. IJPR*, vol. 14, n.º 2, pp. 385–394, 2015.
[32] A. R. Pinho *et al.*, «In Vitro Cytotoxicity Effects of Zinc Oxide Nanoparticles on Spermatogonia Cells», *Cells*, vol. 9, n.º 5, p. 1081, abr. 2020, doi: 10.3390/cells9051081.
[33] P. Talarska, M. Boruczkowski, e J. Żurawski, «Current Knowledge of Silver and Gold Nanoparticles in Laboratory Research—Application, Toxicity, Cellular Uptake», *Nanomaterials*, vol. 11, n.º 9, p. 2454, set. 2021, doi: 10.3390/nano11092454.
[34] C. Carlson *et al.*, «Unique Cellular Interaction of Silver Nanoparticles: Size-Dependent Generation of Reactive Oxygen Species», *J. Phys. Chem. B*, vol. 112, n.º 43, pp. 13608–13619, out. 2008, doi: 10.1021/jp712087m.
[35] A. Steins *et al.*, «Cell death and barrier disruption by clinically used iodine concentrations», *Life Sci. Alliance*, vol. 6, n.º 6, p. e202201875, mar. 2023, doi: 10.26508/lsa.202201875.
[36] S. Chandrasekharan, G. Chinnasamy, e S. Bhatnagar, «Sustainable phyto-fabrication of silver nanoparticles using Gmelina arborea exhibit antimicrobial and biofilm inhibition activity», *Sci. Rep.*, vol. 12, n.º 1, Art. n.º 1, jan. 2022, doi: 10.1038/s41598-021-04025-w.

[37] «The antibacterial effects of gold nanoparticles against E. coli strains», Omnia Health Insights. Acedido: 30 de setembro de 2023. [Em linha]. Disponível em: https://insights.omnia-health.com/laboratory/antibacterial-effects-gold-nanoparticles-against-e-coli-strains